

# A Search for Hydroxylamine ( $\text{NH}_2\text{OH}$ ) toward Select Astronomical Sources

Robin L. Pulliam

*National Radio Astronomy Observatory, Charlottesville, VA 22903, USA*

Brett A. McGuire

*Division of Chemistry and Chemical Engineering, California Institute of Technology  
Pasadena, CA 91125, USA*

Anthony J. Remijan

*National Radio Astronomy Observatory, Charlottesville, VA 22903, USA*

## ABSTRACT

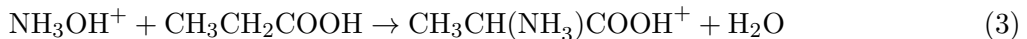
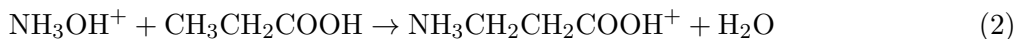
Observations of 14 rotational transitions of hydroxylamine ( $\text{NH}_2\text{OH}$ ) using the NRAO 12 m Telescope on Kitt Peak are reported towards IRC+10216, Orion KL, Orion S, Sgr B2(N), Sgr B2(OH), W3IRS5, and W51M. Although recent models suggest the presence of  $\text{NH}_2\text{OH}$  in high abundance, these observations resulted in non-detection. Upper limits are calculated to be as much as six orders of magnitude lower than predicted by models. Possible explanations for the lower than expected abundance are explored.

## 1. Introduction

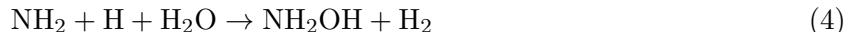
Hydroxylamine ( $\text{NH}_2\text{OH}$ ) has been suggested as a possible reactant precursor in the formation of interstellar amino acids (Blagojevic et al. 2003; Snow et al. 2007). The presence of amino acids in the gas-phase toward astronomical environments would have a profound impact on the effort to understand the origin of complex molecular material in space. The recent discovery of the simplest amino acid glycine ( $\text{NH}_2\text{CH}_2\text{COOH}$ ) in cometary samples collected by the Stardust mission has provided new clues towards our knowledge of the delivery of prebiotic material to planetesimals (Elsila et al. 2009) yet not to their initial formation. That is, are complex prebiotic molecules, such as glycine, formed via reactions of smaller precursors *after* their incorporation into cometary bodies, or do these complex molecules form first in the gas phase before accretion? The search for interstellar, gas-phase glycine has therefore attracted much attention, but has yet to be unambiguously confirmed in space (Kuan et al. 2003; Snyder et al. 2005). Recently, laboratory experiments have shown that ionized  $\text{NH}_2\text{OH}$ , reacting in the gas phase with acetic acid ( $\text{CH}_3\text{COOH}$ ) and propanoic acid ( $\text{CH}_3\text{CH}_2\text{COOH}$ ), can lead to the formation of glycine and the amino acids  $\alpha$ - and  $\beta$ -alanine

( $\text{CH}_3\text{CH}(\text{NH}_2)\text{COOH}$ ) (Blagojevic et al. 2003; Snow et al. 2007). As acetic acid has already been observed in various environments (Shiao et al. 2010 and references therein), the detection of  $\text{NH}_2\text{OH}$  would be of much interest to the astrochemistry community, helping to answer the question of how these large complex molecules form in astronomical environments.

Protonated hydroxylamine,  $\text{NH}_3\text{OH}^+$  and  $\text{NH}_2\text{OH}_2^+$ , is also fundamentally interesting as a prebiotic molecule, having been shown to be a precursor to amino acid formation (Snow et al. 2007). As shown in Equations 1-3, protonated hydroxylamine can react with  $\text{CH}_3\text{COOH}$  (Equation 1) and  $\text{CH}_3\text{CH}_2\text{COOH}$  (Equations 2 and 3) to produce protonated glycine and protonated  $\beta$ - and  $\alpha$ -alanine, respectively. Since  $\text{CH}_3\text{COOH}$  is a well established interstellar molecule, the detection of  $\text{NH}_3\text{OH}^+$  in the ISM would greatly enhance our understanding of the possible formation route to glycine and possibly other simple amino acids in interstellar environments (Mehringer et al. 1997).



There are few laboratory studies of  $\text{NH}_2\text{OH}$  or protonated  $\text{NH}_2\text{OH}$  formation. Nishi et al. (1984) proposed a route for synthesis of  $\text{NH}_2\text{OH}$  involving ice mixtures of water and ammonia where a radical recombination reaction (Equation 4) just above the surface of the ice under irradiated conditions produces  $\text{NH}_2\text{OH}$ .



Additionally, Zheng & Keiser (2010) have recently produced  $\text{NH}_2\text{OH}$  through electron irradiation of water-ammonia ices. They propose that  $\text{NH}_2\text{OH}$  results from the radical recombination of  $\text{NH}_2$  and  $\text{OH}$  inside the ices. The results of both of these studies suggest that radical reactions within ice mantles on grain surfaces may be responsible for  $\text{NH}_2\text{OH}$  production.

In fact, two recent gas-grain chemical models employ such reactions of radicals in their simulations. Charnley et al. (2001) assumed that nitrogen atoms will first react with  $\text{OH}$  in the gas-phase to produce large amounts of  $\text{NO}$  (Equation 5). A fraction of  $\text{NO}$  ( $\sim 10\%$ ) is then accreted onto dust grains where it can then be converted to form species such as  $\text{HNO}$  and  $\text{NH}_2\text{OH}$  through  $\text{H}$  addition reactions. This formation pathway is contingent upon the depletion of  $\text{NO}$  onto dust grains in significant quantities in astronomical environments, though solid evidence for  $\text{NO}$  on grain surfaces is limited. Observational data for the presence of  $\text{NO}$  on grain mantles was first reported in the infrared by Allamandola & Norman (1978) via the fundamental rovibrational band at  $5.3 \mu\text{m}$ . More recently, Akyilmaz et al. (2007) have shown that gas-phase  $\text{NO}$  is depleted towards the peak of dust emission in two sources, suggesting that  $\text{NO}$  has accreted onto the grains in these regions.



Modeling by Garrod et al. (2008) employs a more expansive network of radical-radical reactions within the ice-mantle, incorporating large radicals formed from photolysis of the ice constituents already known to be present. These radical “fragments” go on to react, building more complex species as they become mobile on the grain surface through a gradual warm-up process before being liberated into the gas phase. Formation of  $\text{NH}_2\text{OH}$  is predicted to start from the radical-radical reaction of  $\text{NH} + \text{OH}$  addition on grain surfaces followed by hydrogenation or directly by the reaction of  $\text{OH} + \text{NH}_2$ . The model predicts an  $\text{NH}_2\text{OH}$  column density as high as  $10^{16} \text{ cm}^{-2}$ ; easily within the detectable limits of modern radio telescopes.

Given the potential importance of  $\text{NH}_2\text{OH}$  to prebiotic chemistry and the high predicted abundances, we conducted a search for  $\text{NH}_2\text{OH}$  in the frequency range of 130-170 GHz towards seven sources: IRC+10216, Orion KL, Orion S, Sgr B2(N), Sgr B2(OH), W3IRS5, and W51M. While these sources are known to contain copious amounts of complex molecular material, no definitive evidence was found for  $\text{NH}_2\text{OH}$  toward any of these sources. Upper limits to the beam averaged column density of  $\text{NH}_2\text{OH}$  were calculated based on the  $1\sigma$  rms noise limit of the observed spectra and we discuss possible explanations for the lower than expected abundances.

## 2. Observations

A 2 mm spectral line survey of IRC+10216, Orion KL, Orion S, Sgr B2(N), Sgr B2(OH), W3IRS5, and W51M (hereafter, the Turner 2mm Survey) was conducted using the NRAO<sup>1</sup> 12 m telescope on Kitt Peak by B. E. Turner between 1993 and 1995<sup>2</sup>. Table 1 lists the observing parameters for each source in the survey. Column 1 lists the source; columns 2 and 3 list the reported pointing positions precessed to J2000 coordinates<sup>3</sup>; column 4 reports the observed spectral linewidth in  $\text{km s}^{-1}$  and column 5 lists the assumed source local standard of rest velocity ( $\text{km s}^{-1}$ ) for each source. The frequency range covered by this survey was between 130-170 GHz and the half-power beam width (HPBW) varied from  $38''$ – $46''$  across the band. The observations were taken using a dual channel, SIS junction single side band receiver with typical receiver noise ranging from 75 - 100 K. The backend consisted of a 768 channel, 600 MHz bandwidth hybrid spectrometer with spectral resolution of 0.781 MHz per channel or  $\sim 1.3 \text{ km/s}$  at 150 GHz. The intensity scale at the NRAO 12m is given as  $T_R^*$  and corrects for forward spillover loss. The radiation temperature

---

<sup>1</sup>The National Radio Astronomy Observatory (NRAO) is a facility of the National Science Foundation, operated under cooperative agreement by Associated Universities, Inc.

<sup>2</sup>The survey data are available online (<http://www.cv.nrao.edu/Turner2mmLineSurvey>) with the Spectral Line Search Engine (SLiSE) developed by A. J. Remijan and M. J. Remijan. Further details of the Turner 2mm survey including the motivation for a complete survey of these sources are described in Remijan et al. 2008, arXiv:0802.2273v1 [astro-ph]

<sup>3</sup>The precession from B1950 to J2000 coordinates was done using the FUSE Precession Routine available at: <http://fuse.pha.jhu.edu/support/tools/precess.html>

is defined in Equation 6, where  $\zeta_c$  is the beam efficiency. These data were mined for the all the available 2 mm lines of  $\text{NH}_2\text{OH}$  listed in Table 2.

$$T_R = T_R^*/\zeta_c \quad (6)$$

In total, 54 transitions of  $\text{NH}_2\text{OH}$  are reported between 130 and 170 GHz from the published literature (Müller et al. 2005; Morino et al. 2000; Tsunekawa 1972). Of these 54 transitions, 14 were selected, five *a*-type transitions and nine *c*-type transitions, in this search for having the largest line strength and lowest upper state energy level. Table 2 is a summary of each searched transition and lists the  $\text{NH}_2\text{OH}$  transition rest frequency (column 1), the transition quantum numbers (column 2),  $\theta_b$  is the telescope beam size at the observed frequency (column 3),  $E_u$  is the upper state energy (column 4), the transition type (column 5),  $\text{Log}_{10}(A_{ij})$  is the Einstein A coefficient (column 6) and  $g_{J_u}$  is the *J* degeneracy of the upper state (column 7). Other relevant spectroscopic parameters such as the  $\text{NH}_2\text{OH}$  dipole moments, partition function and rotational constants are listed in the Notes of Table 2.

### 3. Results

Figures 1-3 show the observed spectra (black trace) for each source in the frequency range of the  $\text{NH}_2\text{OH}$  target transitions<sup>4</sup>. Shown in red is a simulated spectrum of the expected transition line strengths from  $\text{NH}_2\text{OH}$  using the total column density predicted for Sgr B2(N) from the Garrod et al. (2008) model and source-appropriate rotational temperatures and line widths (Equation 4). The simulated spectra in red has been scaled down by a factor of 100 for clarity. For illustrative purposes, an unscaled simulation is shown in blue for Sgr B2(N) in Figure 1. While the total column density of  $\text{NH}_2\text{OH}$  in sources other than Sgr B2(N) can be expected to vary based on chemical composition and physical environment, the simulations serve to show in a qualitative sense that the searched for transitions of  $\text{NH}_2\text{OH}$  are not present toward these sources beyond the  $1\sigma$  RMS noise limit and certainly not present in the abundances predicted by the model. In several sources, emission features are present at a number of the appropriate center frequencies for  $\text{NH}_2\text{OH}$ . Yet, the strongest transitions of  $\text{NH}_2\text{OH}$  in this band are the  $J = 3-2$  manifold near 151 GHz and in no source are all of the expected transitions observed. This indicates that the observed emission features are coincidental overlap with other molecular transitions and  $\text{NH}_2\text{OH}$  is not observed in these sources.

Using Equation 7, upper limits to the beam averaged column density based on the  $1\sigma$  RMS noise limit were calculated and are reported in Table 3. An approximate rotational temperature

---

<sup>4</sup>For the purposes of this study, we have not identified the other molecular features within Figures 1-3. The data are publically available (refer to Footnote 2) and we encourage the readers to download the data and use the publically available spectral line databases for assignments.

appropriate for each source was used based on data available in the references shown in Table 3. For the purposes of this work, CH<sub>3</sub>OH was used as a primary source of temperature information when available. CH<sub>3</sub>OH was chosen as it is a well known temperature probe and traces the molecular gas of the desired regions. Additionally, the wealth of observational data on CH<sub>3</sub>OH establishes confidence in temperatures derived from its observations. It should be noted that the upper limits presented here are fairly insensitive to the relatively minor range of rotational temperatures observed in these sources. Fractional abundances with respect to molecular hydrogen were calculated for each source based on these upper limits. In the case of Sgr B2(N), the Garrod et al. (2008) model predicts a relative abundance for NH<sub>2</sub>OH of  $3.5 \times 10^{-7}$  -  $4.2 \times 10^{-6}$ , which is up to six orders of magnitude higher than the observed upper limits (see Table 3).

$$N_{tot} = \frac{8\pi\nu^2 k Q_{rot} \int T_R^* dV}{g_{J_u} g_{k_u} h c^3 A} e^{E_u/kT_{rot}} \quad (7)$$

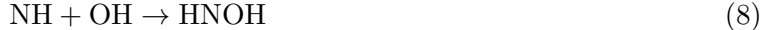
## 4. Discussion

In this paper we reported on the negative detection of hydroxylamine (NH<sub>2</sub>OH) towards several astronomical sources. Upper limits to the beam averaged column density have also been determined for each source based on the  $1\sigma$  RMS noise level in each spectra. Recent chemical models introduced a new gas-grain chemical network utilizing radical-radical reactions as formation mechanisms (Garrod et al. 2008). The model reproduces the beam averaged column densities of species such as methanol (CH<sub>3</sub>OH), acetaldehyde (CH<sub>3</sub>CHO), and even glycolaldehyde (CH<sub>2</sub>(OH)CHO) with excellent agreement with current observed abundances toward the Sgr B2(N) star-forming region (Garrod et al. 2008). However, for NH<sub>2</sub>OH, the predicted abundances are  $3.5 \times 10^{-7}$  -  $4.2 \times 10^{-6}$ , nearly six orders of magnitude higher than the observed upper limit of  $8 \times 10^{-12}$  towards Sgr B2(N) reported in this study. The following sections discuss possible explanations for this surprising difference, focusing on possible formation and destruction mechanisms.

### 4.1. Formation Mechanisms

The formation of NH<sub>2</sub>OH within ice grains was first proposed by Nishi et al. (1984) as shown in Equation 1. Previous experimental attempts to produce NH<sub>2</sub>OH within the gas phase through the reaction of HNO<sup>+</sup> with H<sub>2</sub> have failed (Blagojevic et al. 2003; Lias et al. 1988). The Garrod et al. (2008) grain chemistry model assumes two formation mechanisms for NH<sub>2</sub>OH, both of which assume radical-radical reactions within the grain mantle. In early times, NH<sub>2</sub>OH is formed through the barrierless (see Figure 1 of Garrod et al. 2008) reactions of the hydroxyl radical (-OH) with NH followed by hydrogenation (Equations 8 and 9) similar to the well studied hydrogenation reactions

of CO forming CH<sub>3</sub>OH (Woon 2002).



However, there is no current theoretical or experimental work to suggest this hydrogenation reaction leading to the final product of hydroxylamine in equation (9) proceeds in a manner similar to CO as the model assumes. In fact, given the different states of these molecules, CO having a  $^1\Sigma^+$  electronic configuration while NO is a  $^2\Pi$ , it is likely that the hydrogenation of NO will proceed quite differently from that of CO. This difference could account for the higher abundances predicted by the Garrod et al. (2008) model at lower temperatures. It is also worth bearing in mind that the branching ratios found in the gas phase are not applicable to solid state processes as the surrounding ice can carry away the energy fairly efficiently.

As warming takes place and the hydroxyl radical becomes more mobile on the surface of the grain, the model predicts the barrierless reaction with NH<sub>2</sub> to become dominant (Equation 10).



However, experimental studies have shown (Schnepp & Dressler 1960) that in an isolated argon matrix, NH<sub>2</sub> quickly combines with a free hydrogen radical to form NH<sub>3</sub> when a temperature of 20 K was reached. The question then becomes whether NH<sub>2</sub> and OH have a higher probability to react to form NH<sub>2</sub>OH in interstellar ices before they recombine with free hydrogen to form NH<sub>3</sub> and H<sub>2</sub>O, respectively.

Interstellar ices are considerably more complex than the isolated matrices used in the Schnepp & Dressler (1960) laboratory study, as are the ices considered in the Garrod et al. (2008) model which contain a number of other simple species (e.g. CH<sub>4</sub>, CH<sub>3</sub>OH, NH<sub>3</sub>, CO, CO<sub>2</sub>, HCOOH, H<sub>2</sub>O). As such, NH<sub>2</sub> and OH are not the only species present to react with free hydrogen which may instead react with itself (to form H<sub>2</sub>) or with other smaller species. An examination of the rates of reaction of free hydrogen with these species might therefore be in order to help determine if NH<sub>2</sub> and OH would be available in sufficient quantities to collide and form enough NH<sub>2</sub>OH to be detectable in the ISM. However, the diffusion and evaporation rates of atomic H and other radicals are of more importance. Radical-radical reactions will proceed at the diffusion rates of the reactants and evaporation dominates the loss channels of atomic hydrogen under almost all temperature regimes, which therefore makes it the most important route for determining overall hydrogen populations. Unfortunately, these diffusion rates of reactants are difficult to ascertain experimentally.

There is experimental evidence to support the radical-radical formation of NH<sub>2</sub>OH from NH<sub>2</sub> and OH precursors in electron-irradiated ammonia-water ice samples (Zheng & Kaiser 2010). Upon irradiation, an NH<sub>3</sub> species is found to undergo unimolecular decomposition to form the NH<sub>2</sub> radical and a free hydrogen atom (Equation 11). Water decomposes in a similar fashion, forming OH and

H.



After irradiation, a new absorption peak at  $\sim 1500 \text{ cm}^{-1}$  was observed and attributed to  $\text{NH}_2$  formation. As the ice samples were warmed, the species released in the gas phase were monitored by IR and mass spectroscopy. The presence of  $\text{NH}_2\text{OH}$  was first noted in the IR measurements as the sample reached 174 K. As the temperature continued to rise, the abundance of  $\text{NH}_2\text{OH}$  decreased until non-detection at 200 K.  $\text{NH}_2\text{OH}$  was also observed in the mass spectroscopy measurements from 160 - 180 K. It is important to note that  $\text{NH}_2\text{OH}$  is observed at temperatures above which most, if not all, of the water and ammonia are sublimed.

While this study does support the formation of  $\text{NH}_2\text{OH}$  through radical-radical recombination within interstellar ices, it also provides potential evidence as to why  $\text{NH}_2\text{OH}$  is not currently observed in the ISM. Is there a possible temperature problem? The Garrod et al. (2008) model predicts the high abundance of  $\text{NH}_2\text{OH}$  with a temperature on the order of  $\sim 130 \text{ K}$ .

Zheng & Keiser (2010) find that water, ammonia and hydroxylamine co-desorb, while some  $\text{NH}_2\text{OH}$  remains in the ice samples to somewhat higher temperatures. According to the experimental data,  $\text{NH}_2\text{OH}$  was not observed in the gas phase until temperatures exceeded 160 K. However, temperature programmed laboratory desorption experiments demonstrate behavior that is strongly dependent on the heating rate and this experimentally determined evaporation temperature does not correspond to the actual interstellar value. Without running further analyses of the laboratory data, such as fitting the data to a Polanyi-Wigner type expression (see Galway & Brown 1999 and references therein) or running chemical models, making a qualitative comparison between evaporation temperatures from the lab and in the interstellar medium is difficult.

Also, strong water absorption bands obscure  $\text{NH}_2\text{OH}$  absorption features, making its detection using infrared observations towards hot core regions impossible. However, it is possible the  $\text{NH}_2\text{OH}$  emission is confined to very compact ( $< 5''$ ) hot core regions such as the SgrB2(N-LMH) where the temperatures are higher and hydroxylamine would be completely released from the grain surfaces (Miao et al. 1995). Single dish observations from this survey would be too beam diluted to detect the emission from this compact region. Such an occurrence has been noted before. Acetic acid ( $\text{CH}_3\text{COOH}$ ) has been confirmed in several hot core regions using interferometric observations after searches with single dish observations resulted in negative detections (Wooten et al. 1992; Mehringer et al. 1997; Remijan et al. 2002; Remijan et al. 2003). Additionally, many of the single dish spectra presented here are very dense with molecular emission. Interferometric images have less line confusion than that of single dish. Many of features in single dish spectra arise from an extended region or from different locations within the source and this is demonstrated with the detection of amino acetonitrile by Belloche et al. (2008). The single dish spectra of amino acetonitrile were heavily contaminated with other complex molecular species with only 88 of the 398 observed transitions being reported as relatively "clean". Interferometric observations of Sgr B2(N) confirmed the compact emission of amino acetonitrile with a source

size of 2'' (Belloche et al. 2008). As such, higher spatial resolution interferometric observations may be needed to more thoroughly couple to the higher temperature regions in order to detect hydroxylamine.

Alternatively, observations could be conducted towards molecular sources in shocked regions such as the bipolar outflow L1157(B). In these types of sources, molecules which are formed on grain surfaces but which are not liberated into the gas phase by thermal desorption due to low temperatures are instead ejected into the gas phase by shocks (Requena-Torres et al. 2006). Detection of  $\text{NH}_2\text{OH}$  in these sources would provide valuable insight into the mechanisms behind its formation pathways and eventual release into the gas phase.

## 4.2. Protonated Hydroxylamine

Next we examine possible pathways for the destruction of  $\text{NH}_2\text{OH}$  once it enters the gas phase. It is well known that ion-molecule reactions are important in gas phase interstellar chemistry and that protonated species play an important role in reaction mechanisms.  $\text{NH}_2\text{OH}$ , having a high proton affinity ( $\sim 193.5 \text{ kcal mol}^{-1}$ ) is particularly susceptible to protonation from other species such as  $\text{H}_3^+$ ,  $\text{HCO}^+$ ,  $\text{CH}_5^+$ ,  $\text{H}_3\text{O}^+$  and  $\text{CH}_3\text{OH}_2^+$  (Blagojevic et al. 2003 and references therein). The energies of protonation of  $\text{NH}_2\text{OH}$  by  $\text{H}^+$  and the possibility of proton transfer by  $\text{H}_3^+$  have been predicted by theory (Boulet et al. 1999; Angelelli et al. 1995; Pèrez & Contreras 1998). As a result of protonation, two stable species were reported:  $\text{NH}_3\text{OH}^+$  and  $\text{NH}_2\text{OH}_2^+$ , with  $\text{NH}_3\text{OH}^+$  found to be more stable by  $\sim 100 \text{ kJ mol}^{-1}$ .

The reaction of  $\text{NH}_2\text{OH}$  with either  $\text{H}^+$  or protonated methanol ( $\text{CH}_3\text{OH}_2^+$ ) was predicted to be very exothermic and it was proposed that the excess energy would either dissociate the species or could lead to the rearrangement of the species to the higher energy  $\text{NH}_2\text{OH}_2^+$ . This could result in an enhanced abundance of  $\text{NH}_2\text{OH}_2^+$  in the ISM. Once in the gas phase, recent theoretical work has shown that the reaction of ionized and protonated  $\text{NH}_2\text{OH}$  with  $\text{H}_2$ , its most likely collision partner, is highly unfavorable (Largo et al. 2009). These species, therefore, are likely to remain as reaction partners for further chemistry.

Given these considerations, even if  $\text{NH}_2\text{OH}$  is produced on ice grains through radical-radical reactions, upon its release into the gas phase it may quickly undergo protonation. This would result in very low observed abundances of  $\text{NH}_2\text{OH}$  in the ISM. Once protonated, the reaction with  $\text{H}_2$ , by far the most likely collision partner, is highly unfavorable and the lifetimes of these species should therefore be greatly enhanced. A search for  $\text{NH}_2\text{OH}_2^+$  and  $\text{NH}_3\text{OH}^+$  within these star forming regions might be prudent; although, dissociative recombination reactions could result in lowered abundances of these species. This would first require the acquisition of the rotational spectra of these species in the laboratory to enable astronomical searches.



## 5. Conclusion

We report the non-detection of  $\text{NH}_2\text{OH}$  towards seven sources. Calculated upper limits for the abundance of this molecule are as much as six orders of magnitude lower than those predicted for the species by recent models. Several factors could account for this discrepancy including the rapid removal of precursor molecules from ice mantles through reaction with free hydrogen or the rapid protonation (and subsequent dissociative recombination) of  $\text{NH}_2\text{OH}$  by  $\text{H}^+$ ,  $\text{H}_3^+$ ,  $\text{CH}_5^+$ , and other efficient protonation mechanisms. The single dish observations presented here are likely highly beam diluted. Higher resolution interferometric observations could provide the sensitivity required for detection and therefore allow better refinement of models which currently predict the presence of  $\text{NH}_2\text{OH}$  in high abundance.

BAM gratefully acknowledges G.A. Blake for his support, as well as funding by an NSF Graduate Research Fellowship. We also would like to thank the anonymous reviewer for the valuable comments and suggestions to improve the quality of the paper.

Table 1. Observed sources and coordinates (J2000), spectral line widths, and  $v_{LSR}$  for each source.

Source	RA	Dec	$\Delta V$ (km s <sup>-1</sup> )	$v_{LSR}$ (km s <sup>-1</sup> )
Orion KL	05 35 14.5	-05 22 32.6	4.5	+9 <sup>a</sup>
Orion S	05 35 16.5	-05 19 26.7	4.5	+7 <sup>b</sup>
IRC+10216	09 47 57.3	+13 16 43.0	9.0	-26 <sup>c</sup>
Sgr B2(OH)	17 47 20.8	-28 23 32.2	9.0	+60 <sup>d</sup>
Sgr B2(N)	17 44 11.0	-28 22 17.3	9.0	+62 <sup>e</sup>
W51M	19 16 43.8	+14 30 07.5	9.0	+57 <sup>f</sup>
W3IRS5	02 27 04.1	+61 52 21.4	9.0	-39 <sup>g</sup>

References. —

- a) (Ziurys & McGonagle 1993)  
b) (Menten et al. 1988) c) (Latter & Charnley 1996)  
d) (Turner 1991) e) (Nummelin et al. 2000)  
f) (Millar et al. 1988) g) (Helmich et al. 1994)

Table 2. Observed transitions of  $\text{NH}_2\text{OH}$ , beam size, and parameters used to simulate the spectra and calculate  $\text{NH}_2\text{OH}$  beam averaged column densities (see Equation 4).

Rest Frequency (MHz)	Transition $J_u(K_a K_c) - J_l(K_a K_c)$	$\theta_b$ ( $\mu$ )	$E_u$ ( $\text{cm}^{-1}$ )	Type	$\text{Log}_{10}(A_{ij})$ ( $\text{s}^{-1}$ )	$g_{J_u}$
151020.70	3(1,3)-2(1,2)	41.52	10.57	a	-5.27587	7
151101.99	3(2,2)-2(2,1)	41.50	27.16	a	-5.47928	7
151102.32	3(2,1)-2(2,0)	41.50	27.16	a	-5.47928	7
151117.67	3(0,3)-2(0,2)	41.49	5.04	a	-5.22390	7
151207.01	3(1,2)-2(1,1)	41.47	10.57	a	-5.27422	7
164340.78	9(1,9)-9(0,9)	38.15	75.59	c	-7.02982	19
164627.49	8(1,8)-8(0,8)	38.09	60.48	c	-7.02783	17
164883.24	7(1,7)-7(0,7)	38.03	47.04	c	-7.02617	15
165107.71	6(1,6)-6(0,6)	37.98	35.28	c	-7.02472	13
165300.63	5(1,5)-5(0,5)	37.93	25.2	c	-7.02335	11
165461.76	4(1,4)-4(0,4)	37.89	16.8	c	-7.02237	9
165590.89	3(1,3)-3(0,3)	37.87	10.08	c	-7.02148	7
165687.89	2(1,2)-2(0,2)	37.84	5.04	c	-7.02079	5
165752.62	1(1,1)-1(0,1)	37.83	1.68	c	-7.02037	3

Note. — a) Molecular data were obtained from the Cologne Database for Molecular Spectroscopy (Müller et al. 2005) available at [www.splatalogue.net](http://www.splatalogue.net) (Remijan & Markwick-Kemper 2008). The uncertainties of the transition frequencies are 50 kHz (Morino et al. 2000).

b) Degeneracies calculated as:  $g_{J_u} = 2J + 1$ ,  $g_{K_u=0} = 1$ ,  $g_{K_u \neq 0} = 2$

c) Rotational constants from the CDMS Database:

$A = 190976.2$  MHz,  $B = 25218.73$  MHz,  $C = 25156.66$  MHz

d)  $\text{NH}_2\text{OH}$  dipole moments in Debye (Müller et al. 2005):  $\mu_A=0.589$ ;  $\mu_C=0.060$

e) The functional form of the rotational partition function was determined from Equation 3.69 of Gordy & Cook (Third Ed., 1984) -  $Q_{rot}=0.5T_{rot}^{1.5}$  and confirmed by a fit to the partition function data given in (Müller et al. 2005).

Table 3.  $1\sigma$  RMS level of  $T_R^*$ , upper limits on column density of  $\text{NH}_2\text{OH}$ ,  $\text{H}_2$  column density, relative abundance of  $\text{NH}_2\text{OH}$ , and assumed value of  $T_{rot}$ .

Source	$T_R^*$ (mK)	$N_{\text{NH}_2\text{OH}}$ ( $\text{cm}^{-2}$ )	$N_{\text{H}_2}$ ( $\text{cm}^{-2}$ )	$N_{\text{NH}_2\text{OH}}/N_{\text{H}_2}$	$T_{rot}$ (K)
Orion KL <sup>a</sup>	6.4	$<2 \times 10^{13}$	$7.0 \times 10^{23}$	$<3 \times 10^{-11}$	120
Orion S <sup>b</sup>	4.0	$<9 \times 10^{12}$	$1.0 \times 10^{23}$	$<9 \times 10^{-11}$	80
IRC+10216 <sup>c</sup>	5.1	$<8 \times 10^{13}$	$3.0 \times 10^{22}$	$<3 \times 10^{-9}$	200
Sgr B2(OH) <sup>d</sup>	7.0	$<3 \times 10^{13}$	$1.0 \times 10^{24}$	$<3 \times 10^{-11}$	70
Sgr B2(N) <sup>e</sup>	6.6	$<2 \times 10^{13}$	$3.0 \times 10^{24}$	$<8 \times 10^{-12}$	70
W51M <sup>f</sup>	7.7	$<4 \times 10^{13}$	$1.0 \times 10^{24}$	$<4 \times 10^{-11}$	100
W3IRS5 <sup>g</sup>	4.3	$<2 \times 10^{13}$	$5.0 \times 10^{23}$	$<3 \times 10^{-11}$	70

References. —

- a)  $T_{rot}$  from (Ziurys & McGonagle 1993);  $N_{\text{H}_2}$  from (Womack et al. 1992) and Refs. therein.
- b)  $T_{rot}$  from (Menten et al. 1988);  $N_{\text{H}_2}$  from (Womack et al. 1992) and Refs. therein.
- c)  $T_{rot}$  from (Patel et al. 2011);  $N_{\text{H}_2}$  from (Cernicharo et al. 2010)
- d)  $T_{rot}$  from (Turner 1991);  $N_{\text{H}_2}$  from (Womack et al. 1992) and Refs. therein.
- e)  $T_{rot}$  and  $N_{\text{H}_2}$  from (Nummelin et al. 2000)
- f)  $T_{rot}$  from (Millar et al. 1988);  $N_{\text{H}_2}$  from (Womack et al. 1992) and Refs. therein.
- g)  $T_{rot}$  and  $N_{\text{H}_2}$  from (Helmich et al. 1994)

Fig. 1.— Observed  $a$ -type transitions of  $\text{NH}_2\text{OH}$  are simulated in red over the observed spectrum in black. Simulated spectra are shown divided by a factor of 100. An unscaled simulation is shown in blue for Sgr B2(N) for illustrative purposes.

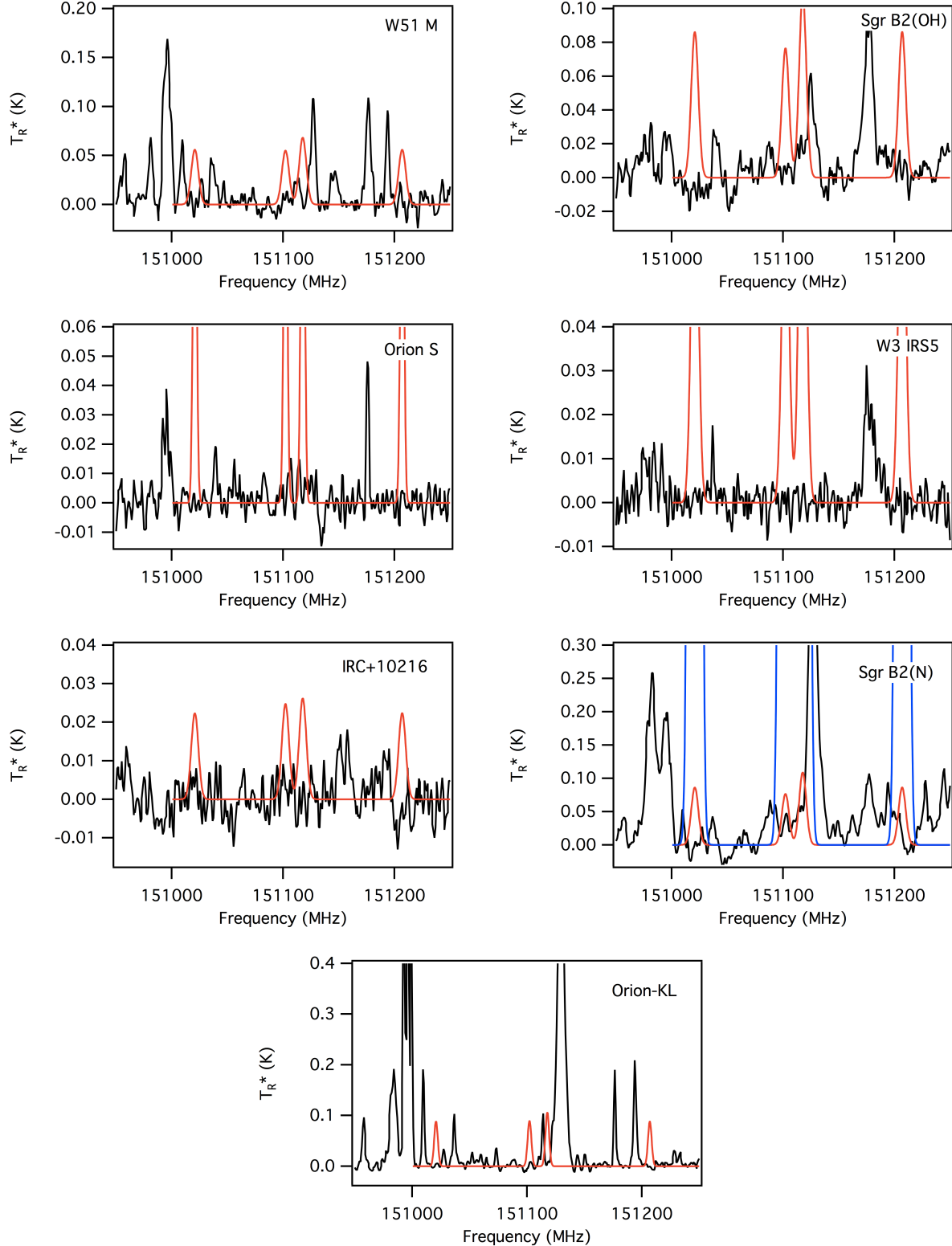


Fig. 2.— Observed  $c$ -type transitions of  $\text{NH}_2\text{OH}$  are simulated in red over the observed spectrum in black. No scaling factor has been applied to the simulated spectra.

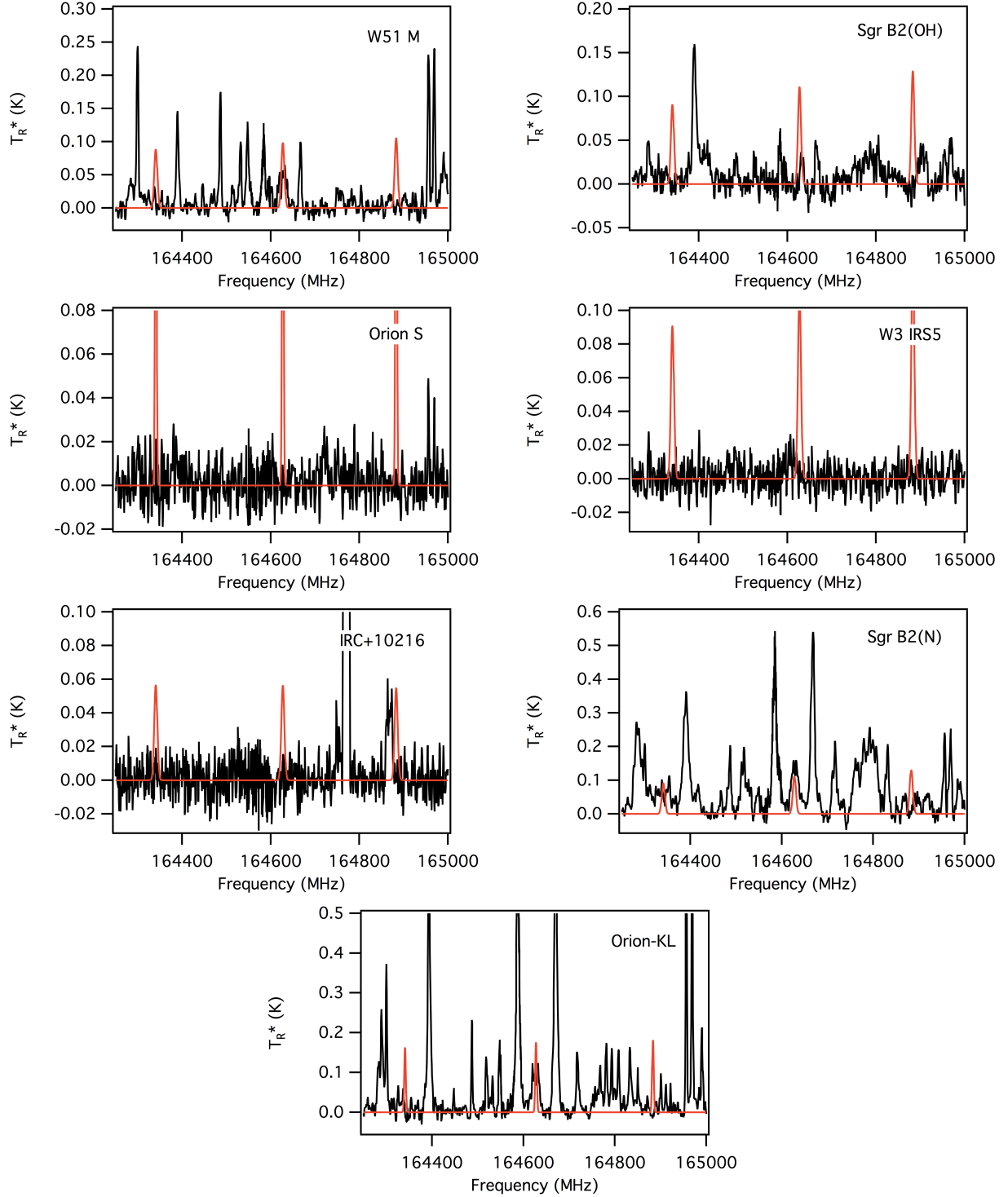
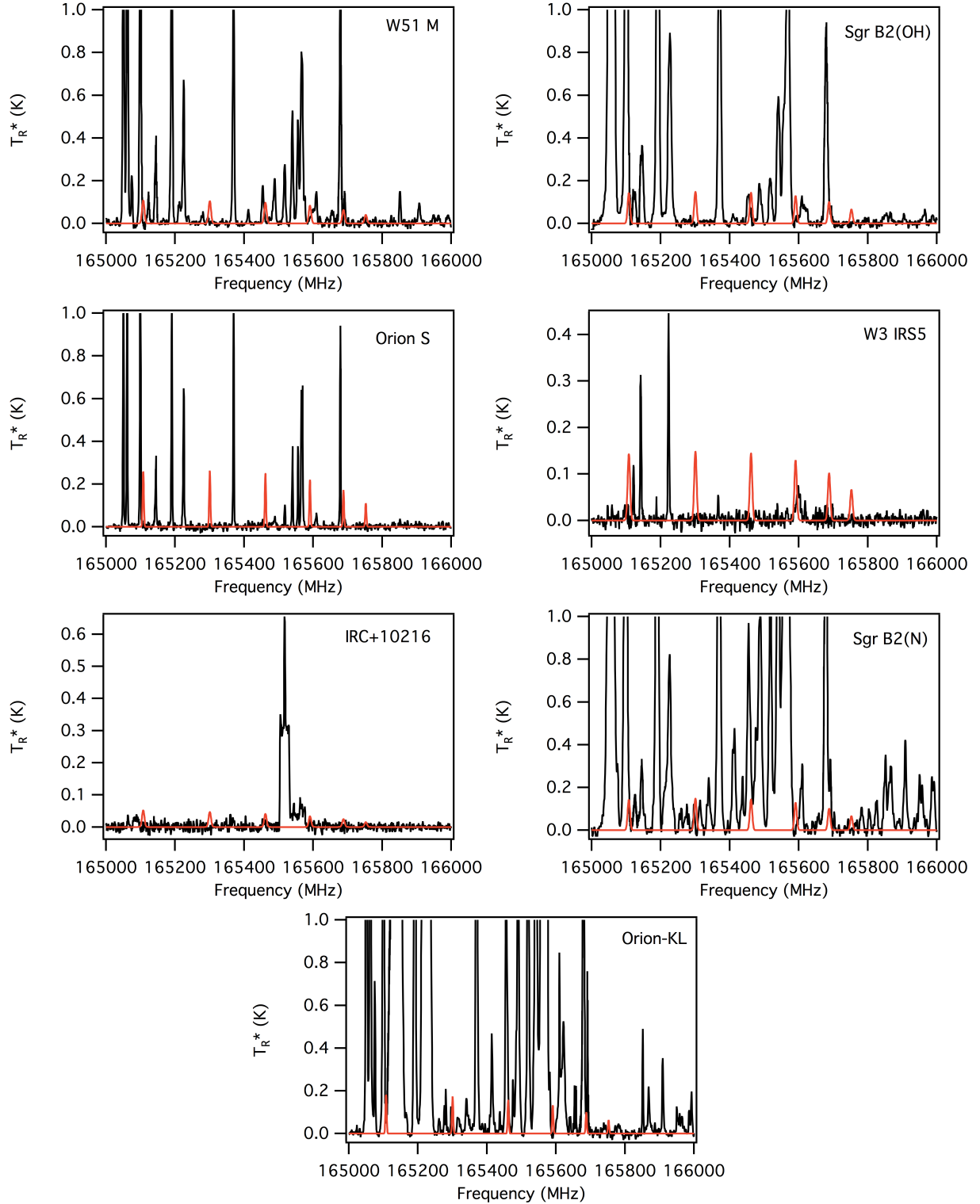


Fig. 3.— Observed *c*-type transitions of  $\text{NH}_2\text{OH}$  are simulated in red over the observed spectrum in black. No scaling factor has been applied to the simulated spectra.



## REFERENCES

- Akyilmaz, M., Flower, D.R. Hily-Blant, P., Pineau es Forêts, G., & Walmsley, C.M., 2007 *Astron. & Astrophys.*, **462**, 221.
- Allamandola, L.J. & Norman, C.A., 1978 *Astron. & Astrophys.*, **63**, L23.
- Angelelli, F., Aschi, M., Cacace, F., Pepi, F., & de Petris, G., 1995 *J. Phys. Chem.*, **99**, 6551.
- Belloche, A., Menten, K.M., Comito, C., Müller, H.S.P., Schilke, P. , Ott, J., Thorwirth, S., & Hieret, C., 2008, *Astron. & Astrophys.*, **482**, 179.
- Blagojevic, V., Petrie, S., & Bohme, D.K., 2003 *M. N. R. A. S.*, **339**, L7.
- Boulet, P., Gilardoni, F., Weber, J., Chermette, H., & Ellinger, Y., 1999 *Chem. Phys.*, **244**, 163.
- Cernicharo, J., Waters, L.B.F.M., Decin, L., & Encrenaz, P. et al., 2010 *Astron. & Astrophys.*, **521**, L8.
- Charnley, S.B., Rodgers, S.D., & Ehrenfreund, P., 2001 *Astron. & Astrophys.*, **378**, 1024.
- Elsila, J.E., Glavin, D.P., & Dworkin, J.P., 2009 *Meteor. & Planet. Sci.*, **44**, 1323.
- Flower, D.R., Pineau des Forets, G., & Walmsley, C.M., 2005 *Astron. & Astrophys.*, **436**, 933.
- Galway, A.K., & Brown, B.E. 1999, *Thermal Decomposition of Ionic Solids*, Elsevier: New York, NY, 123.
- Garrod, R.T., Widicus Weaver, S.L., & Herbst, E., 2008 *Astrophys. J.*, **682**, 283.
- Gordy, W., & Cook, R.L. 1984, *Microwave Molecular Spectra*, Third Ed., Wiley-Interscience: New York, NY, 58.
- Helmich, F.P., Jansen, D.J., de Graauw, Th., Groesbeck, T.D., & van Dishoeck, E.F., 1994 *Astron. & Astrophys.*, **283**, 626.
- Herbst, E. & Leung, C. M., 1986 *M. N. R. A. S.*, **222**, 689.
- Kuan, Y.J., Charnley, S.B., Huang, H.C., Tseng, W.L., & Kisiel, Z., 2003 *Astrophys. J.*, **593**, 848.
- Largo, L., Rayón, V.M., Barrientos, C., Largo, A., & Redondo, P., 2009 *Chem. Phys. Lett.*, **476**, 174.
- Latter, W.B. & Charnley, S.B., 1996 *Astrophys. J.*, **463**, L37.
- Lias, S.G., Barmess, J.E., & Liebman, J.F. et al., 1988 *J. Phys. Chem. Ref. Dat.*, **17** (Supplement 1), 1.
- McGonagle, D., Ziruyz, L.M., Irvine, W. M., & Minh, Y. C., 1990 *Astrophys. J.*, **359**, 121.



- Mehringner, D.M., Snyder, L.E., Miao, Y.T., & Lovas, F.J., 1997 *Astrophys. J.*, **480**, L71.
- Menten, K.M., Walmsley, C.M., Henkel, C., & Wilson, T.L., 1988 *Astron. & Astrophys.*, **198**, 253.
- Miao, Y., Mehringer, D.M., Kuan, Y., & Snyder, L.E., 1995 *Astrophys. J.*, **445**, L59.
- Millar, T.J., Olofsson, H., Hjalmarsen, Å., & Brown, P.D., 1988, *Astron. & Astrophys.*, **205**, L5.
- Morino, I., Yamada, K.M.T., Klein, H., & Belov, S.P. et al., 2000 *J. Mol. Struct.*, **517-518**, 367.
- Müller, H.S.P., Schlöder, F., Stutzki, J., & Winnewisser, G., 2005 *J. Mol. Struct.*, **742**, 215.
- Nishi, N., Shinohara, H., & Okuyama, T., 1984 *J. Chem. Phys.*, **80**, 3898.
- Nummelin, A., Bergman, P., & Hjalmarsen, Å., et al., 2000 *Astrophys. J. Suppl.*, **128**, 213.
- Patel, N.A, Young, K.H., & Gottlieb, C.A., et al., 2011 *Astrophys. J. Suppl.*, **193**, 17.
- Pèrez, P. & Contreras, R., 1998 *Chem. Phys. Lett.*, **293**, 239.
- Ragan, S.E., Bergin, E.A., & Wilner, D., 2011 *Astrophys. J.*, **736**, 163.
- Remijan, A.J., Snyder, S.-Y.L., Liu, S.-Y., Mehringer, D., & Kuan, Y.-J., 2002 *Astrophys. J.*, **576**, 264.
- Remijan, A.J., Snyder, S.-Y.L., Friedel, D.N., Liu, S.-Y., & Shah, R.Y., 2003 *Astrophys. J.*, **590**, 314.
- Remijan, A.J., Hollis, J.M., Lovas, F.J., Stork, W.D., Jewell, P.R., & Meier, D.S., 2008 *Astrophys. J.*, **675**, L85.
- Remijan, A.J., & Markwick-Kemper, A.J., 2008, *Bull. of the Am. Astron. Soc.*, **39**, 963.
- Requena-Torres, M.A., Martin-Pintado, J., Rodriguez-Franco, A., Martin, S., Rodriguez-Fernandez, N.J., & de Vicente, P., 2006 *Astron. & Astrophys.*, **455**, 971.
- Schnepp, O. & Dressler, K., 1960 *J. Chem. Phys.*, **32**, 1682.
- Shiao, Y.S.J., Looney, L.W., Remijan, A.J., Snyder, L.E., & Friedel, D.N., 2010 *Astrophys. J.*, **716**, 286.
- Snow, J.L., Orlova, G., Blagojevic, V., & Bohme, D.K., 2007 *J. Am. Chem. Soc.*, **129**, 9910.
- Snyder, L.E., Lovas, F.J., & Hollis, J.M., et al., 2005 *Astrophys. J.*, **619**, 914.
- Tsunekawa, S., 1972 *J. Phys. Soc. Japan*, **33**, 167.
- Turner, B.E., 1991 *Astrophys. J. Suppl.*, **76**, 617.
- Woon, D.E., 2002 *Astrophys. J.*, **569**, 541.

- Wooten, A., Wlodarczack, G., Mangum, J.G., Combes, F., Encrenaz, P.J., & Gerin, M., 1992 *Astron. & Astrophys.*, **257**, 740.
- Zheng, W.J. & Kaiser, R.L., 2010 *J. Phys. Chem. A.*, **114**, 5251.
- Ziurys, L.M. & McGonagle, D., 1993 *Astrophys. J. Suppl.*, **89**, 155.
- Womack, M., Ziurys, L.M., & Wyckoff, S., 1992 *Astrophys. J.*, **393**, 188.